Therapeutics, Targets, and Chemical Biology

Cancer Research

Anti–αv Integrin Monoclonal Antibody Intetumumab Enhances the Efficacy of Radiation Therapy and Reduces Metastasis of Human Cancer Xenografts in Nude Rats

Shoucheng Ning[1], Junqiang Tian[1], Deborah J. Marshall[2], and Susan J. Knox[1]

Abstract

We previously reported that intetumumab (CNTO 95), a fully human anti–αv integrin monoclonal antibody, is a radiosensitizer in mice with xenograft tumors. Because intetumumab does not cross-react with mouse integrins, but has cross-reactivity with rat integrins, we next studied the potential combined use of radiation therapy and intetumumab in human cancer xenograft models in nude rats to assess effects on both tumor cells and the tumor microenvironment. Nude rats bearing human head and neck cancer and non–small cell lung cancer (NSCLC) xenografts were treated with intetumumab and fractionated local tumor radiotherapy. Effects on tumor growth and metastasis, blood perfusion, oxygenation, and gastrointestinal toxicity were studied. Intetumumab alone had a moderate effect on tumor growth. When combined with fractionated radiation therapy, intetumumab significantly inhibited tumor growth and produced a tumor response rate that was significantly better than with radiation therapy alone. Treatment with intetumumab also significantly reduced lung metastasis in the A549 NSCLC xenograft model. The oxygenation and blood perfusion in xenograft tumors measured by microbubble-enhanced ultrasound imaging were substantially increased after treatment with intetumumab. The combined use of intetumumab and radiation therapy reduced the microvessel density and increased apoptosis in tumor cells and the tumor microenvironment. Toxicity studies showed that treatment with intetumumab did not cause the histopathologic changes in the lungs and did not sensitize the sensitive gastrointestinal epithelium to the effect of radiation therapy. Intetumumab can potentiate the efficacy of fractionated radiation therapy in human cancer xenograft tumors in nude rats without increased toxicity.
Cancer Res; 70(19); 7591–9. ©2010 AACR.

Introduction

Intetumumab (CNTO 95) is a fully human anti–αv integrin monoclonal antibody that binds human αv integrin–expressing cells with high affinity (K_d, approximately 1–24 nmol/L) and has limited cross-reactivity with rat αv integrin (K_d, 220 nmol/L; ref. 1). Preclinical studies have shown that intetumumab exhibits antiangiogenic and antitumor activity in human cancer xenograft models in nude mice (1–3). Intetumumab has been reported to inhibit cell adhesion, migration, invasion, and proliferation of endothelial cells and tumor cells *in vitro* and tumor metastasis *in vivo* in nude mice with human breast cancer xenografts by inactivating the focal adhesion kinase (FAK) and the docking protein paxillin (1, 4). We have previously shown that intetumumab is a potential radiation sensitizer when used in combination with fractionated radiation therapy in human cancer xenograft models in nude mice (5). Data from two multicenter clinical phase I studies in patients with advanced solid tumors have shown that intetumumab was safe and well tolerated either alone or in combination with docetaxel (6, 7). Intetumumab is now in phase II clinical trials for the treatment of a variety of malignancies.

Although the specific mechanism of action responsible for the antitumor activity of intetumumab has been not fully elucidated, inhibition of tumor angiogenesis via inhibitory effects on targeted integrins is thought to play an important role in the inhibition of tumor growth. However, the antitumor and antimetastatic activities of intetumumab observed in nude mice with human cancer xenografts are most likely independent of its antiangiogenic activity because intetumumab does not cross-react with mouse αv integrins. In fact, intetumumab was more potent in inhibiting tumor growth in nude rats than in nude mice with the same human melanoma xenografts (1). To fully assess the effects of intetumumab on radiation response of tumors and interaction of tumor cells and their microenvironments, we next studied the combined use of intetumumab and fractionated local tumor radiation therapy in nude rats with human cancer xenograft. Based on our previous studies (5, 8, 9), we hypothesized that intetumumab would potentiate the efficacy of fractionated radiation

Authors' Affiliations: [1]Department of Radiation Oncology, Stanford University Medical Center, Stanford, California and [2]Centocor, Inc., Radnor, Pennsylvania

Corresponding Author: Susan J. Knox, Department of Radiation Oncology, Stanford University Medical Center, 269 Campus Drive, CCSR South 1245, Stanford, CA 94305-5152. Phone: 650-723-5832; E-mail: sknox@stanford.edu.

doi: 10.1158/0008-5472.CAN-10-1639

therapy and inhibit tumor metastasis by blocking the function of adhesion molecules in the microenvironment of potential metastatic sites.

Materials and Methods

Antibodies

Intetumumab (CNTO 95) was provided by Centocor, Inc. Intetumumab was diluted in physiologic saline (0.9% sodium chloride) at a concentration of 1.0 mg/mL for i.p. injection.

Cell culture

Human head and neck cancer cell lines FaDu and non–small cell lung cancer (NSCLC) cell line A549 were obtained from the American Type Culture Collection. Cells were maintained in DMEM (Invitrogen) supplemented with 10% FCS, 100 units/mL penicillin, and 100 μg/mL streptomycin in a 37°C humidified incubator with a mixture of 95% air and 5% CO_2. All experiments were performed on exponentially growing cells with a cell population doubling time of approximately 24 to 36 hours. The identity of cells has regularly been confirmed throughout the course of the studies by observation of the growth pattern and cell morphology *in vitro* and *in vivo*.

Rat tumor model and therapy

Male nude rats, 5 to 6 weeks old and 150 to 200 g in body weight, were purchased from Harlan Laboratories. Rats were tested and found to be negative for specific pathogens. The rats were normally bred and maintained under specific pathogen-free conditions, and sterilized food and water were available *ad libitum*. Rats were injected s.c. in the right flank with 5×10^6 tumor cells in a suspension volume of 0.1 mL. One tumor per rat was inoculated. When tumors reached an average size of 200 mm^3 (150–250 mm^3), rats were randomly assigned to the different treatment groups. Intetumumab was injected i.p. at a dose of 10 mg/kg body weight, once weekly until completion of the study, or as specified in each experiment. In combination therapy, intetumumab was injected 30 to 60 minutes before irradiation. For irradiation, the anesthetized tumor-bearing rats were placed in individual lead boxes with tumors protruding through a cutout window at the rear of each box. The radiation was delivered using a Philips RT-250 200 kVp X-ray unit (12.5 mA; half-value layer, 1.0-mm Cu) at a dose rate of 140 cGy/min. Tumors were locally irradiated with a dose of 250 cGy per fraction daily for 5 consecutive days. In some experiments, a single dose of irradiation was used as specified in each experiment. The length and width of the tumors were measured with calipers before treatment, and three times a week thereafter until the tumor volume reached at least four times the pretreatment volume. The tumor volume was calculated using the formula: tumor volume (mm^3) = $\pi/6 \times \text{length} \times \text{width}^2$. The response of tumors to the treatment is defined as complete response (CR), partial response (PR), stable disease (SD), and progressive disease (PD). A CR of tumors was recorded if a tumor completely disappeared and was not palpable at the end of the experiment (or 30 days after completion of radiation therapy). A PR was a reduction in volume of ≥50% compared with the initial tumor volume at the start of treatment. SD was defined as the tumor size neither PR nor PD criteria met. PD was an increase in tumor volume of ≥20% of the pretreatment volume. Body weight of animals was measured three times a week. The animal experiments described herein were approved by the Stanford University Administrative Panel for Laboratory Animal Care.

Lung metastasis models

We studied the lung metastasis of tumors using two different tumor metastasis models: an i.v. injection model and a s.c. tumor model. In the i.v. injection model, nude rats were injected with 1×10^6 A549 cells in 0.2-mL Hank's solution via the lateral tail vein. Immediately after tumor cell injection, rats were randomly assigned to two groups. One group of nine rats was injected i.p. with 10 mg/kg intetumumab, once a week for 60 days. A second group of 10 rats was injected with physiologic saline (10 mL/kg), once weekly for 60 days.

In the s.c. tumor model, nude rats were inoculated s.c. in the right flank with 5×10^6 A549 cells, with one tumor site per rat. When tumors reached an average size of 200 mm^3, rats were randomly assigned to one of four treatment groups and treated as described above in the Rat tumor model and therapy section. After 60 days, rats were euthanized and the lungs were immediately removed and fixed in either Bouin's solution or 10% buffered formalin for counting of pulmonary metastatic nodules.

Immunohistochemistry analysis

General histopathologic changes, apoptosis, and microvessel density of tumors were assessed by immunohistochemical staining. Tumor-bearing rats were euthanized 3 days after treatment for tumor collection with three rats per treatment regimen. Harvested tumors were immediately frozen in OCT compound, sectioned at 8-μm thickness, and stained with H&E for general histopathologic analysis, with an ApopTag peroxidase *in situ* oligo ligation (ISOL) apoptosis detection kit (Chemicon International) for detection of apoptosis, and with an anti-CD31 polyclonal antibody (Santa Cruz Biotechnology) for microvessel density counts. Slides were counterstained with hematoxylin for background nuclear visualization. Slides were visualized and photographed using a Leica DM6000B fluorescence/light microscope (Leica Microsystems). For quantification of microvessels, tissue sections were analyzed at ×40 magnification and CD31-positive vessels were counted. Four fields per section were randomly analyzed, and data are presented as the mean ± SD of three tumors.

Assessment of tumor hypoxia

Tumor hypoxia was assessed using the hypoxia marker EF5 as previously described (10). Briefly, 3 days after treatment with a single dose of 10 mg/kg intetumumab or 5 Gy irradiation alone, or in combination, rats bearing FaDu tumors were injected with 10 mmol/L EF5 solution. Two hours later, tumors were collected, frozen in liquid nitrogen, sectioned, and stained with anti-EF5 antibody ELK3-51 conjugated with

Cy3. Digital photomicrographs were taken at ×40 magnification with a fluorescence microscope. The Cy3 signal was analyzed with Adobe Photoshop program. The EF5 binding due to hypoxia was determined by correction for nonspecific and endogenous binding.

Microbubble-enhanced ultrasound image

Two days after treatment, tumor-bearing rats were imaged on a Vevo 770 system (VisualSonics, Inc.) with a 40-MHz transducer. Rats were anesthetized with a 3% isoflurane-oxygen mixture, and the body temperature was monitored and maintained at 37°C on a warming plate during the imaging session. The coupling gel was applied to the skin over the tumor, and a 12 × 12–mm view field was imaged by two-dimensional contrast mode. A baseline image was acquired before microbubble injection. The contrast-enhanced image was acquired 5 seconds after a bolus injection of the non-targeted microbubble contrast agent (3×10^8 microbubbles/0.1 mL) via a tail vein catheter. Images were acquired at 20 frames per second for a total of 800 frames. The image data were analyzed using Vevo 770 Contrast Mode software by comparing the contrast cine loop with the baseline cine loop to generate a contrast overlay to identify the differences in image intensity between these two loops.

Intestinal crypt stem cell assay

Nude rats were divided into two groups. One group of rats was injected i.p. with a single dose of 10 mg/kg intetumumab 1 hour before irradiation. Rats were irradiated with a total body irradiation (TBI) at doses of 10 to 15 Gy. There were three rats per dose point per group. Three days following irradiation, rats were euthanized. The duodenum, jejunum, and ileum were immediately removed and fixed in 10% buffered formalin. The intestinal segments were cut into four pieces, embedded in paraffin, sectioned, and stained with H&E. Surviving crypts (≥10 cells) for each cross-section were counted by light microscopy. Each viable crypt is presumed to contain one or more surviving intestinal crypt stem cells. Eight cross-sections were scored per segment. The results are presented as mean crypt cell numbers per cross-section ± SD.

Statistics

Data were statistically analyzed using a two-tailed Student's *t* test.

Results

Effect of intetumumab on tumor responses to local fractionated radiation therapy

Nude rats with established FaDu and A549 xenograft tumors were treated with (*a*) 10 mg/kg intetumumab, once a week; (*b*) 250 cGy radiation daily for 5 days; (*c*) a combination of intetumumab and radiation as above; or (*d*) an i.p. injection of normal saline (0.01 mL/g body weight) once weekly as an untreated control. Data are shown in Table 1 and Fig. 1. Treatment with intetumumab alone, radiotherapy alone, or in combination inhibited tumor growth and produced complete regression of tumors in both FaDu and A549 tumor models. The total tumor response rates (CR and PR) were 33%, 67%, and 89% in FaDu tumor model and 17%, 17%, and 67% in A549 tumor model for intetumumab alone, radiation alone, and combination therapy, respectively. The combination treatment was more effective in inhibiting tumor growth and resulted in complete regression of tumors in seven of nine rats with FaDu tumors and four CRs of six rats with A549 tumors, which was significantly higher than the other treatment regimens studied ($P < 0.05$). In addition, tumors with a PR and no response (SD and PD) to the treatment grew slower following combined therapy than those treated with either intetumumab or radiation alone (Fig. 1).

Table 1. Therapeutic responses of FaDu and A549 xenograft tumors in nude rats

Tumor model	No. animal	Tumor response				CR + PR (% total)
		CR	PR	SD	PD	
FaDu						
Untreated control	9			1	8	0
Intetumumab alone	9	3			6	33
Radiation alone	9	6			3	67
Intetumumab + radiation	9	7	1		1	89
A549						
Untreated control	6				6	0
Intetumumab alone	6	1			5	17
Radiation alone	6	1		2	3	17
Intetumumab + radiation	6	4		2		67

NOTE: CR, complete disappearance of tumors on day 30; PR, ≥50% decrease in tumor volume on day 30; SD, no significant change in tumor volume on day 30; PD, ≥20% increase in tumor volume on day 30.

Intetumumab alone or in combination with radiation did not cause any significant decrease in body weight compared with untreated control animals (data not shown). There were no obvious change in the general appearance, skin reaction, or daily activity of tumor-bearing rats treated with intetumumab either alone or in combination with radiation. H&E staining of the lungs showed that there were no obvious changes in histopathology in lungs from rats treated with intetumumab either alone or in combination with radiation compared with untreated control animals.

Effect of intetumumab on tumor metastasis

Next, we studied the effects of intetumumab on the lung metastasis of A549 xenograft tumors using an i.v. injection model for testing the homing ability of lung cancer cells and a s.c. tumor model for testing the spontaneous metastasis to lung. Data are shown in Fig. 2. There were significant differences in the number of rats with metastatic lung lesions and the mean number of metastatic lesions per lung between

the intetumumab-treated group and the untreated control group. Sixty days after an i.v. injection of A549 cells, 9 of 10 rats developed metastatic lung lesions in the untreated control group, whereas only 4 of 9 rats developed lung metastases in the intetumumab-treated group ($P < 0.05$). The average number of metastatic lesion per lung was 56 ± 50 (with a range of 3–142) in the control group and 13 ± 8 (with a range of 6–24) in the intetumumab-treated group ($P = 0.02$).

In the s.c. tumor model, treatment with intetumumab alone or in combination with local tumor radiation inhibited spontaneous lung metastasis of A549 tumors and decreased both the number of rats with lung metastasis and the number of metastatic lesions per lung (Fig. 2). The average number of metastatic lesions per lung was 18 ± 9, 6 ± 2, 12 ± 9, and 4 ± 2 for groups treated with normal saline (control), intetumumab alone, radiation alone, and the combination of intetumumab and radiation, respectively.

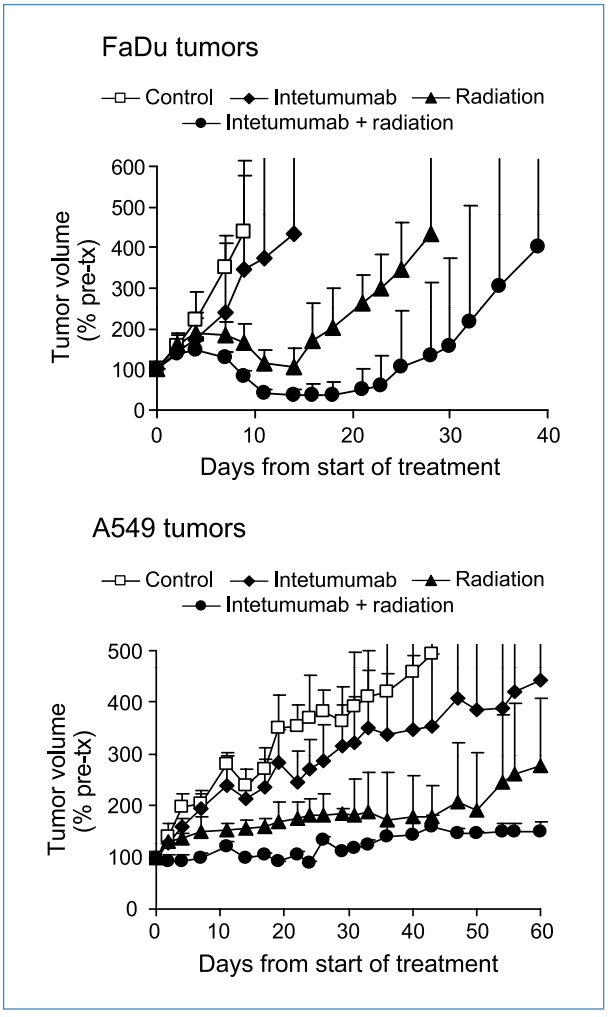

Figure 1. Tumor growth curves of FaDu and A549 xenograft tumors in nude rats. There were four groups: (*a*) untreated control; (*b*) intetumumab, 10 mg/kg weekly; (*c*) 250 cGy radiation daily for 5 d; and (*d*) combination of intetumumab and radiation. Six to nine nude rats were used in each group. In combination therapy, intetumumab was injected 30 to 60 min before irradiation. Points, average tumor volume of each group versus time from start of treatment; bars, SD. Tumors with complete regression to the treatment were not included.

Effect of intetumumab on apoptosis, microvasculature, oxygenation, and blood perfusion of xenograft tumors

To understand the mechanism of action by which intetumumab enhances the efficacy of radiation therapy, we studied apoptosis, microvessel density, oxygenation, and blood perfusion in xenograft tumors using immunohistochemical staining (Fig. 3) and microbubble-enhanced micro-ultrasound imaging (Fig. 4).

The apoptotic cell death in tumors was assessed using the ApopTag peroxidase ISOL apoptosis detection staining. Intetumumab alone did not induce obvious ISOL-positive apoptotic cell staining. The ISOL-positive apoptotic cells were much more evident in tumors treated with radiation either alone or in combination with intetumumab. The mean number of apoptotic cells per view field was 8 ± 4 for the untreated control, 9 ± 3 for intetumumab alone, 52 ± 5 for radiation alone, and 116 ± 12 for the combination of intetumumab and radiation ($P < 0.01$, combination versus all other groups), respectively.

CD31 staining showed that intetumumab alone did not significantly affect the number of CD31-positive microvessel compared with untreated control tumors (28 ± 2 per field for control and 25 ± 5 per field for intetumumab alone; $P = 0.3$), but morphologically, vessels in intetumumab-treated tumors were more regular and distributed more uniformly than seen in untreated control tumors. Radiation therapy reduced the number of CD31-positive microvessel to 13 ± 2 per field (a 54% decrease; $P = 0.03$ versus control). The combination of radiation and intetumumab further reduced the number of tumor microvessels to 6 ± 2 per field, representing a further 54% decrease ($P = 0.02$ versus radiation alone). Morphologically, the microvessels were much less regular and shorter and had more closed ends in tumors treated with radiation, either alone or in combination with intetumumab.

Results of EF5 staining showed that tumors from untreated rats had the highest level of EF5 staining, and tumors from rats treated with the combination of intetumumab and radiation had the lowest EF5 staining (i.e., the lowest level of hypoxia). EF5-stained hypoxic regions were decreased by 40% in tumors treated with intetumumab alone and by 54% in tumors treated with intetumumab and radiation compared with untreated control tumors ($P = 0.01$). The quantification of EF5 staining showed that the EF5 signal intensity was 59 ± 6% that of control tumors in intetumumab-treated tumors, 72 ± 8% in radiation-treated tumors, and 46 ± 6% in tumors treated with intetumumab plus radiation.

To further examine whether the reduction of hypoxia was due to the improvement of blood perfusion in tumors, we assessed the blood perfusion and blood volume in tumors using microbubble-enhanced ultrasound imaging. Figure 4 shows signal intensity as a function of image frame (time), with the slope of the curve representing the relative rate of blood perfusion and the plateau representing the relative blood volume in the tumors. Treatment with intetumumab

dramatically increased the rates of blood perfusion and blood volume of tumors. Radiation alone did not increase the perfusion rate. When combined with intetumumab, the perfusion rate and blood volume in tumors were significantly enhanced.

Meanwhile, H&E staining revealed many more large and diffuse areas of necrosis in tumors treated with radiation, either alone or in combination with intetumumab. There was no apparent difference in the H&E staining of intetumumab-treated tumors and untreated control tumors.

Effect of intetumumab on the sensitivity of intestinal crypt stem cells to radiation—gastrointestinal toxicity study

Gastrointestinal toxicity caused by radiation limits the therapeutic dose that can be used for treating abdominal and pelvic tumors with radiation therapy. This toxicity is primarily due to the killing of the crypt stem cells in the intestinal epithelium. We performed experiments to study the effect of intetumumab on irradiated intestinal crypt cell survival. The results are shown in Fig. 5. Intetumumab alone had no effect on crypt cell growth and proliferation. For radiation, there was a dose-dependent decrease in the crypt stem cells in the duodenum, jejunum, and ileum after a single dose of 10 to 15 Gy TBI. Administration of intetumumab slightly decreased the mean number of surviving crypt cells at radiation doses above 13 Gy. However, the decrease in the mean number of crypt cells was not significantly different when compared with similarly irradiated control rats without intetumumab treatment ($P > 0.05$).

Discussion

We previously reported that intetumumab sensitized human xenograft tumors to radiation in mice (5). Intetumumab does not bind to mouse αv integrins, so this observed effect was due to direct effects of the antibody on the tumor cells, as well as to possible indirect effects of the intetumumab-treated tumor cells on the surrounding vasculature and microenvironment. Therefore, the use of mouse models for these studies was suboptimal because they did not allow for assessment of the direct effect of the antibody on both tumors and tumor vasculature in the tumor microenvironment when combined with radiation. Intetumumab does

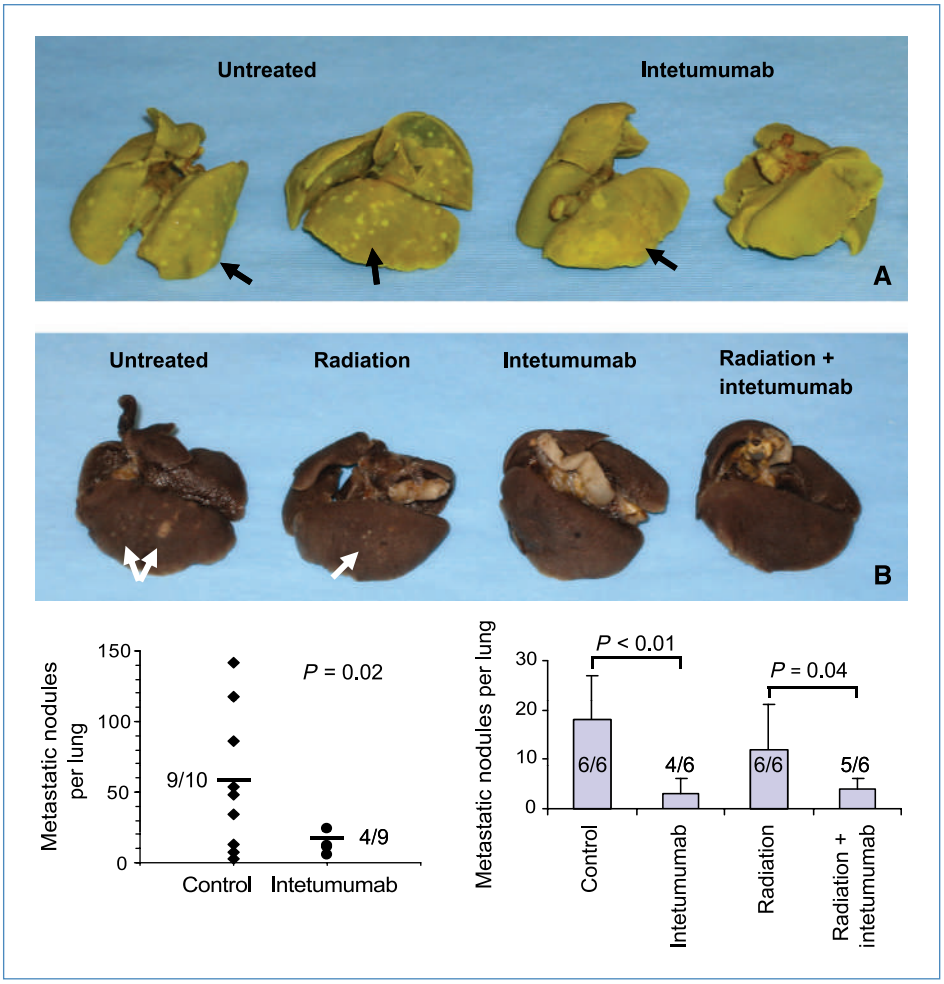

Figure 2. Lung metastasis from i.v. injected A549 tumor cells (A) or from established s.c. A549 tumors in nude rats (B). There were two groups in the i.v. injection model and four groups in the s.c. tumor model. Bottom, quantification of the pulmonary nodules. The numbers in each column indicate the number of rats that developed metastatic pulmonary nodules out of the total number of rats injected with tumor cells.

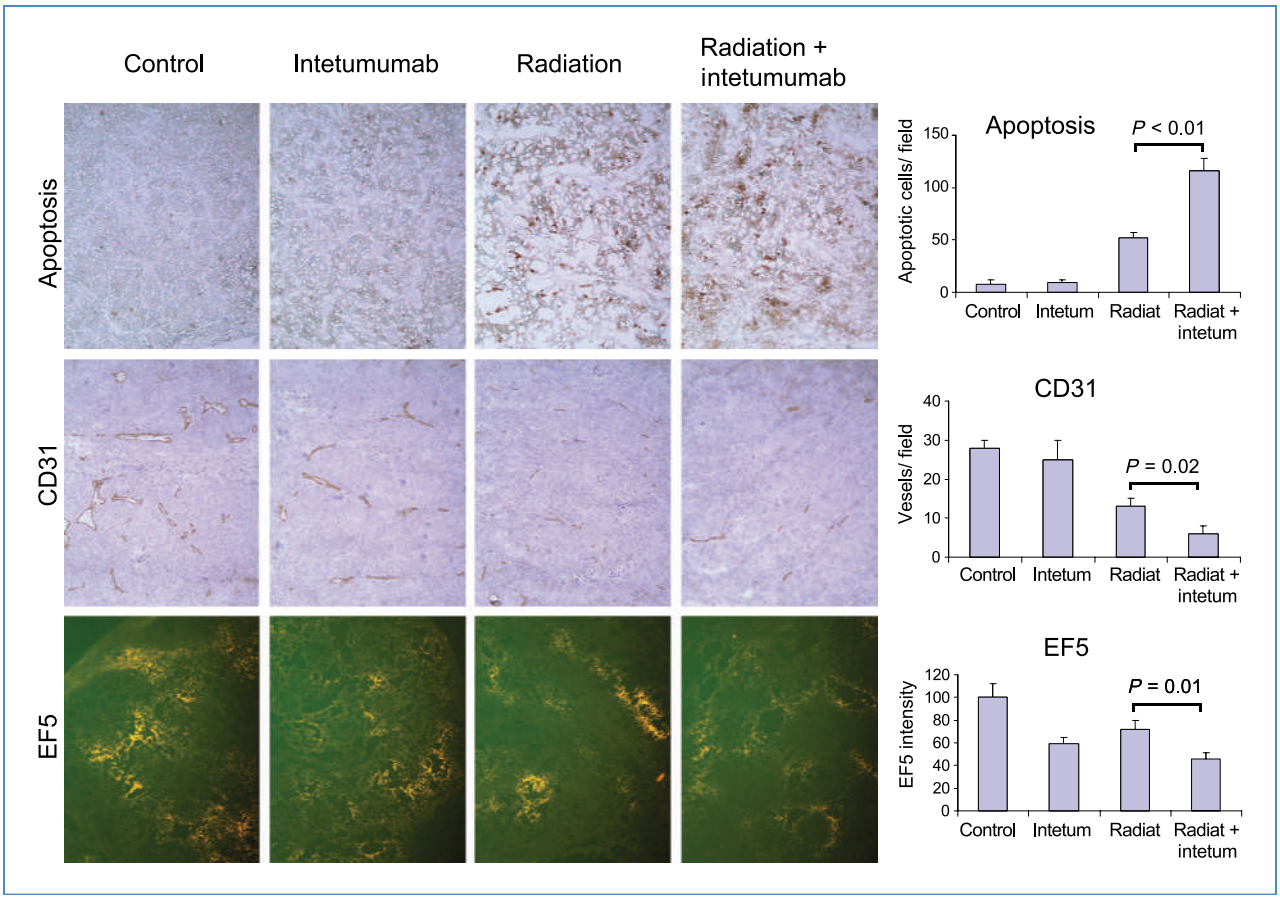

Figure 3. Immunohistochemical analysis of apoptosis, vessel density, and oxygenation in FaDu xenograft tumors. Digital photographs were taken at ×40 magnification with a Leica microscope equipped with a digital camera. Right, quantification of apoptosis, CD31, and EF5 staining. Four fields per section per tumor were analyzed. Columns, mean of three tumors for each group; bars, SD.

cross-react with rat integrins, so to better study the combined effect of intetumumab and radiation in a more clinically relevant model, we used nude rats with well-established human head and neck cancer and NSCLC xenograft tumors for efficacy, toxicity, metastasis, and mechanistic studies.

Intetumumab significantly enhanced the efficacy of radiation in both human head and neck cancer FaDu and NSCLC A549 tumor models. The magnitude of sensitization was greater in these rat models than previously observed with the mouse tumor models, as evidenced by the higher tumor response rates. Although the tumor xenograft models studied in mice and rats differed, we did not previously observe any complete regressions of tumors from four different tumor models studied in mice, including a head and neck tumor model, treated with more frequent dosing of intetumumab (10 mg/kg, three doses per week in mice compared with weekly dose in rats). This was not surprising because in the rat tumor models, the antibody was able to bind to both αv integrin–expressing tumor cells and vascular endothelial cells, and exert direct effects on both.

A variety of mechanistic studies were performed to further elucidate the underlying mechanism of this effect. Microvessels in intetumumab-treated tumors were morphologically more regular and relatively uniformly distributed within the tumors. The combination of intetumumab and radiation resulted in a significant decrease in the microvessel density compared with radiation alone and was associated with morphologic changes indicative of altered vascular function. There was also a correlation between microvessel density and the level of apoptosis in treated tumors. EF5 staining of hypoxic cells was decreased by 40% in tumors treated with intetumumab alone and reduced by 54% in tumors treated with intetumumab plus radiation. Furthermore, microbubble-enhanced ultrasound imaging showed that intetumumab markedly increased tumor blood volume and perfusion rates, which were further enhanced, but to a lesser extent, by combining intetumumab with radiation. Jain (11) has reported that antiangiogenic agents can transiently normalize tumor vasculature and that this effect may be secondarily associated with changes in tumor perfusion and oxygenation. We hypothesize that intetumumab had a similar effect, which is also consistent with results from studies of a variety of other antiangiogenic agents that have been reported to affect microvessel density, morphology, and function and to enhance

tumor responses to radiation (5, 12, 13). Our previous study has shown that treatment with intetumumab inhibited the expression of the angiogenic marker vascular endothelial growth factor receptor in vascular endothelial cells as well as in tumor cells (5). Radiation, on the other hand, not only kills tumor cells and endothelial cells in tumors but also induces and activates the expression of a variety of proangiogenic and prosurvival factors. Treatment with intetumumab in combination with radiation could inhibit the radiation-induced overexpression of proangiogenic factors and angiogenesis in tumors. Taken together, these results suggest that intetumumab inhibited angiogenesis, normalized the microvessel morphology, increased the tumor perfusion rate and blood volume, and increased oxygenation, all of which were further enhanced by radiation, resulting in decreased tumor hypoxia/increased tumor pO_2 and, over time, in increased damage to the tumor microvasculature and increased tumor cell killing.

Although the antiangiogenic and radiosensitizing effects of intetumumab are not unique, intetumumab has the added advantage over many other antiangiogenic agents in development, such as inhibiting the development of metastases by targeting the αv integrin receptors and blocking its downstream cell adhesion signaling pathway (4). Here, we further show the ability of intetumumab to inhibit the subsequent development of pulmonary metastases in the NSCLC A549 model following either i.v. administration of tumor cells or spontaneous metastasis from established s.c. tumors. Metastasis of a primary tumor to distant sites is a complicated multistep process, involving dissociation of tumor cells from the original tumors, epithelial-mesenchymal transition, breach of the basement membrane, invasion of the extracellular matrix tissues, intravasation into preexisting and newly formed blood and lymph vessels (angiogenesis and lymphangiogenesis), transport through and extravasation from vessels, invasion, adhesion, establishment of disseminated cells at a secondary distant site, and proliferation (reviewed in refs. 14, 15). At each step, there are one or more physiologic barriers to the metastasis of tumor cells, such as anoikis, a type of cell death due to detachment or loss of cell adhesion. Studies have shown that integrins play a pivotal role in many steps of this metastatic process, especially in dissociation, invasion, adhesion, proliferation, and angiogenesis in both primary and distant secondary sites (16–20). Integrins, as the key cell surface receptors for cell-cell and cell–extracellular matrix interactions, sense and initiate the signaling of cell motility, invasion, and adhesion; interact with receptor tyrosine kinases; and activate downstream signaling of FAK and SRC family kinases (21). Treatment with intetumumab inactivates the FAK and paxillin docking protein by tyrosine dephosphorylation of the tyrosine residues, followed by the inhibition of invasion and motility of tumor cells *in vitro* (4). Furthermore, intetumumab has been reported to be more potent at inhibiting cell adhesion, motility, and invasion than other anti–αv-containing integrin antibodies, RGD mimetics, and small molecules (1, 4). Interaction of tumor cells with extracellular matrix via adhesion molecules is important for survival and metastasis of tumors and may play a pivotal role in resistance to radiation therapy (22, 23). In addition, the relative radioresistance of stem or stem-like metastatic tumor cells is an important clinical problem (24, 25) and contributes to the failure of conventional cytotoxic therapies. Therefore, one can hypothesize that intetumumab could both block homing of tumor cells to potential metastatic sites and radiosensitize these cells. These properties of intetumumab could potentially inhibit metastasis and facilitate eradication of these resistant tumor subpopulations by radiation, thereby increasing the efficacy of local tumor radiation therapy via multiple mechanisms.

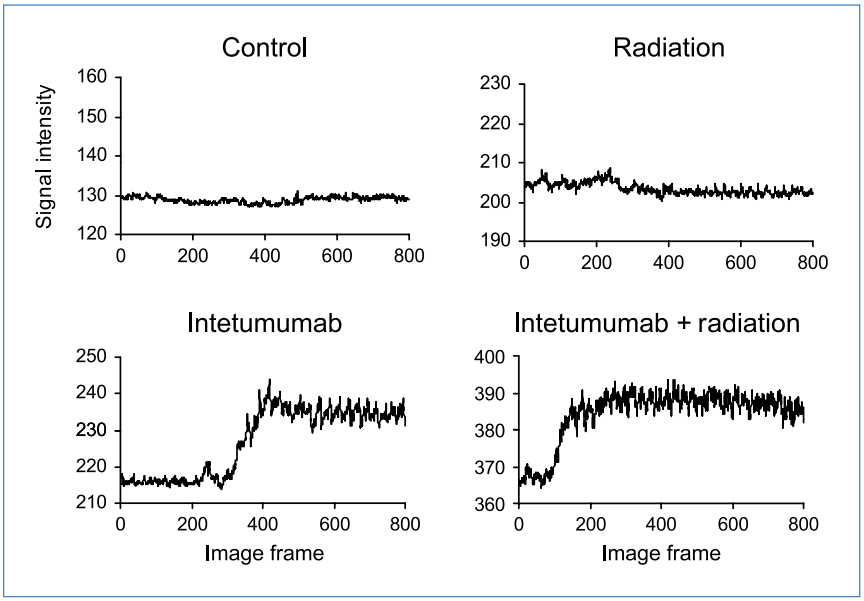

Figure 4. Microbubble-enhanced ultrasound imaging of FaDu tumors in nude rats 2 d after treatment. Data are presented as the image intensity as a function of image frame (time). The first 100 frames were acquired before microbubble injection.

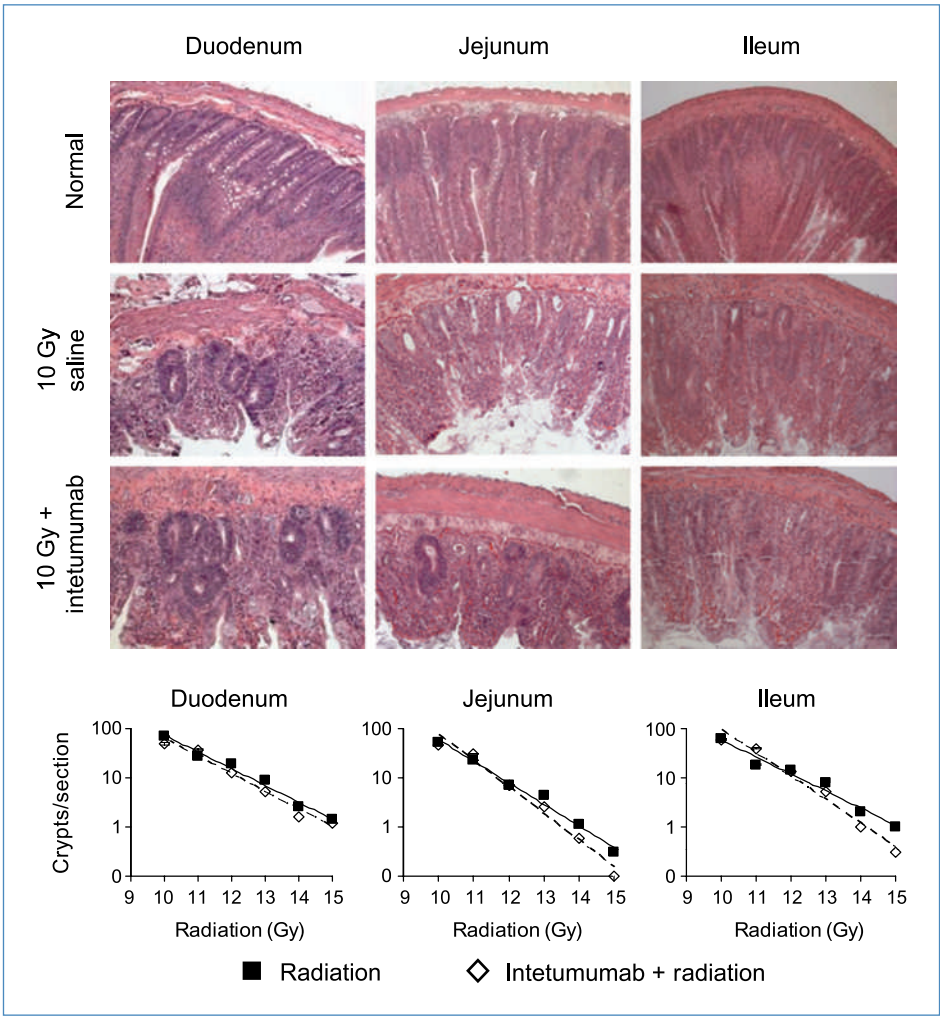

Figure 5. Intestinal crypt stem cell assay. Nude rats were irradiated with TBI with or without preadministration of a single dose of 10 mg/kg intetumumab. Intestinal segments were harvested 3 d after irradiation. Top, representative pictures of H&E-stained intestinal tissue section of normal rats and rats treated with either 10 Gy radiation alone or 10 Gy radiation plus intetumumab. Bottom, quantification of intestinal crypt stem cells. Points, mean of crypt cells per cross-section as a function of radiation dose (in Gy); bars, SD. Solid line and black square, radiation only; dashed line and diamond, radiation plus intetumumab.

Agents that enhance the efficacy of radiation therapy are only beneficial if they do not similarly sensitize normal tissue to radiation therapy. Using the intestinal crypt cell assay, we were able to show that intetumumab alone had no detectable cytotoxic effect on crypt cell numbers or morphology and had no significant effect on the sensitivity of the crypt cells to radiation. This is very important because crypt cells are very radiosensitive, and the sensitivity of the intestines and rectum to radiation limits the dose of radiation that can safely be used to treat abdominal and pelvic tumors. In addition, there were no apparent histopathologic changes in lungs from rats treated with intetumumab either alone or in combination with radiation compared with untreated rats. Intetumumab was very well tolerated by the rats, with no significant weight loss or observable signs of toxicity when used alone or in combination with radiation therapy. It should be pointed out that there is a ubiquitous expression of αv integrins in normal tissues, and the binding of intetumumab to human αv integrins is greater than in rats. Therefore, caution should be used in extrapolating these safety and toxicity data from rats to human patients. However, data from a preclinical toxicity study in cynomolgus macaques showed that treatment with intetumumab produced no sign of toxicity and no histopathologic changes in any of the tissues examined (2). Data from two recently completed phase I clinical trials (6, 7) further showed that intetumumab was generally safe and well tolerated either alone or in combination with docetaxel in 6-week or prolonged treatment regimens. There were no dose-limiting toxicities reported in these studies.

In summary, these results are very encouraging and show that intetumumab can potentiate the efficacy of fractionated radiation therapy and inhibit metastasis in rats with human cancer xenograft tumors, without enhancing effects of radiation on intestinal crypt cells (normal tissue toxicity). These findings may have near-term translational potential for the treatment of solid tumors in patients using radiation therapy.

Disclosure of Potential Conflicts of Interest

No potential conflicts of interest were disclosed.

Received 05/12/2010; revised 07/07/2010; accepted 07/17/2010; published OnlineFirst 09/14/2010.

References

1. Trikha M, Zhou Z, Nemeth JA, et al. CNTO 95, a fully human monoclonal antibody that inhibits αv integrins, has antitumor and antiangiogenic activity *in vivo*. Int J Cancer 2004;110:326–35.
2. Martin PL, Jiao Q, Cornacoff J, et al. Absence of adverse effects in cynomolgus macaques treated with CNTO 95, a fully human anti-αv integrin monoclonal antibody, despite widespread tissue binding. Clin Cancer Res 2005;11:6959–65.
3. Chen Q, Millar H, McCabe FL, et al. αv integrin-targeted immunoconjugates regress established human tumors in xenograft models. Clin Cancer Res 2007;13:3689–95.
4. Chen Q, Manning CD, Millar H, et al. CNTO 95, a fully human anti αv integrin antibody, inhibits cell signaling, migration, invasion, and spontaneous metastasis of human breast cancer cells. Clin Exp Metastasis 2008;25:139–48.
5. Ning S, Nemeth JA, Hanson RL, Forsythe K, Knox SJ. Anti-integrin monoclonal antibody CNTO 95 enhances the therapeutic efficacy of fractionated radiation therapy *in vivo*. Mol Cancer Ther 2008;7:1569–78.
6. Mullamitha SA, Ton NC, Parker GJM, et al. Phase I evaluation of a fully human anti-αv integrin monoclonal antibody (CNTO 95) in patients with advanced solid tumors. Clin Cancer Res 2007;13:2128–35.
7. Chu FM, Picus J, Fracasso PM, Dreicer R, Lang Z, Foster B. A phase I, multicenter, open-label study of the safety of two dose levels of a human monoclonal antibody to human α(v) integrins, intetumumab, in combination with docetaxel and prednisone in patients with castrate-resistant metastatic prostate cancer. Invest New Drugs 2010. Epub ahead of print.
8. Ning S, Laird D, Cherrington JM, Knox SJ. Anti-angiogenic agents SU5416 and SU6668 increase antitumor effects of fractionated irradiation. Radiat Res 2002;157:45–51.
9. Ning S, Chen Z, Dirks A, et al. Targeting integrins and PI3K/Akt-mediated signal transduction pathways enhances radiation-induced anti-angiogenesis. Radiat Res 2007;168:125–33.
10. Ning S, Hartley C, Molineux G, Knox SJ. Darbepoietin alfa potentiates the efficacy of radiation therapy in mice with corrected or uncorrected anemia. Cancer Res 2005;65:284–90.
11. Jain RK. Normalization of tumor vasculature: an emerging concept in antiangiogenic therapy. Science 2005;307:58–62.
12. Li L, Wartchow CA, Danthi SN, et al. A novel antiangiogenesis therapy using an integrin antagonist or anti-Flk-1 antibody coated 90Y-labeled nanoparticles. Int J Radiat Oncol Biol Phys 2004;58:1215–27.
13. Willett CG, Kozin SV, Duda DG, et al. Combined vascular endothelial growth factor-targeted therapy and radiotherapy for rectal cancer: theory and clinical practice. Semin Oncol 2006;33:S35–40.
14. Geiger TR, Peeper DS. Metastasis mechanisms. Biochim Biophys Acta 2009;1796:293–308.
15. Brooks SA, Lomax-Browne HJ, Carter TM, Kinch CE, Hall DM. Molecular interactions in cancer cell metastasis. Acta Histochem 2010;112:3–25.
16. Staflin K, Krueger JS, Hachmann J, et al. Targeting activated integrin αvβ3 with patient-derived antibodies impacts late-stage multiorgan metastasis. Clin Exp Metastasis 2010;27:217–31.
17. Hood JD, Cheresh DA. Role of integrins in cell invasion and migration. Nat Rev Cancer 2002;2:91–100.
18. Hwang R, Varner J. The role of integrins in tumor angiogenesis. Hematol Oncol Clin N Am 2004;18:991–1006.
19. Calabrese C, Poppleton H, Kocak M, et al. A perivascular niche for brain tumor stem cells. Cancer Cell 2007;11:69–82.
20. Ellis SJ, Tanentzapf G. Integrin-mediated adhesion and stem-cell-niche interactions. Cell Tissue Res 2010;339:121–30.
21. Guo W, Giancotti FG. Integrin signaling during tumor progression. Nat Rev Mol Cell Biol 2004;5:816–26.
22. Baluna RG, Eng TY, Thimas CR. Adhesion molecules in radiotherapy. Radiat Res 2006;166:819–31.
23. Sandfort V, Koch U, Cordes N. Cell adhesion-mediated radioresistance revisited. Int J Radiat Biol 2007;83:727–32.
24. Bao S, Wu Q, McLendon RE, et al. Glioma stem cells promote radioresistance by preferential activation of the DNA damage response. Nature 2006;444:756–60.
25. Folkins C, Man S, Xu P, Shaked Y, Hicklin DJ, Kerbel RS. Anticancer therapies combining antiangiogenic and tumor cell cytotoxic effects reduce the tumor stem-like cell fraction in glioma xenograft tumors. Cancer Res 2007;67:3560–4.